

Network Hawkes Process Models for Exploring Latent Hierarchy in Social Animal Interactions

Owen G. Ward*, Jing Wu*, Tian Zheng

Department of Statistics, Columbia University, New York, NY.

Anna Smith

Department of Statistics, University of Kentucky.

James Curley

Department of Psychology, University of Texas at Austin

Summary. Group-based social dominance hierarchies are of essential interest in animal behavior research. Studies often record aggressive interactions observed over time, and models that can capture such dynamic hierarchy are therefore crucial. Traditional ranking methods summarize interactions across time, using only aggregate counts. Instead, we take advantage of the interaction timestamps, proposing a series of network point process models with latent ranks. We carefully design these models to incorporate important characteristics of animal interaction data, including the winner effect, bursting and pair-flip phenomena. Through iteratively constructing and evaluating these models we arrive at the final cohort Markov-Modulated Hawkes process (C-MMHP), which best characterizes all aforementioned patterns observed in interaction data. We compare all models using simulated and real data. Using statistically developed diagnostic perspectives, we demonstrate that the C-MMHP model outperforms other methods, capturing relevant latent ranking structures that lead to meaningful predictions for real data.

Keywords: Animal Behaviour, Hawkes Processes, Latent Ranking, Network Point Processes, Social Hierarchy

1. Introduction

In this paper we consider the problem of providing a general framework for modeling hierarchy among a group of mice through their observed repeated aggressive interactions. We do this using data from the study conducted by Williamson et al. (2016), in order to answer the unsolved questions in that work. Describing the dominance structure of such interactions well is a difficult task. Section 2 presents an overview of existing well-known methods for dominance ranking and their properties. These existing methods suffer several common issues, including the inability to rigorously evaluate the estimated ranking and the inability to deal with the temporal component of these interactions. Specifying statistical generative models therefore provides a natural way to characterize the structure of these social groups more generally. One focus of the models we develop

*These authors contributed equally. Correspondence should be addressed to: Tian Zheng, 1255 Amsterdam Avenue, MC 4690, New York, NY 10027; tzheng@stat.columbia.edu.

here is the ability to capture the temporal and network dynamics of the social dominance hierarchy. In Section 3, we take advantage of the timestamps of these interactions and propose three network point process models: the cohort Hawkes process model (C-HP), the cohort degree corrected Hawkes process model (C-DCHP) and the cohort Markov-modulated Hawkes process model (C-MMHP). We construct these models such that these point processes are a function of a set of latent rank variables. These latent rank variables are a powerful feature of our models, allowing us to incorporate various known characteristics of animal behavior into our model. We develop these models in a Bayesian framework to capture uncertainty estimates and to better model pairs which contain few interactions. We iteratively develop each model from the previous to better account for dynamics seen in animal data. This results in our final Cohort-Markov Modulated Hawkes Process (C-MMHP) model. In Section 4, these models are compared, using simulated and real data, to existing methods for understanding animal dominance ranking. We illustrate that our final model is flexible and adequately captures dynamics of dominance hierarchy by showing results on rank inference, prediction performance and residual analysis. Section 5 summarizes this work and discuss future directions for our proposed model.

2. Background

Here we review the literature on social hierarchy for group-living animals. Empirical studies of the social hierarchy of animals that live in a group are generally developed based on the observations of dyadic, or pairwise, agonistic interactions. In Williamson et al. (2016), the agonistic interactions include fighting, chasing and mounting behaviors. We consider all such aggressive interactions without differentiating the type. We denote the interactions between N animals as a matrix W , where W_{ij} is the number of aggressive interactions initiated by animal i towards animal j . In So et al. (2015) and Williamson et al. (2016), this is also called a *win/loss* matrix.

Two approaches are generally considered in the animal behavior literature to analyse this win/loss matrix (Drews, 1993): *functional* methods and *structural* methods. *Functional* methods aim to directly infer a ranking of animals from this win/loss matrix by rearranging this matrix in an attempt to best capture behavioral patterns, expected in a social hierarchy. The rank is therefore inferred directly from the observations recorded in the *win/loss* matrix. If $W_{ij} > W_{ji}$ then functional methods infer that i dominates j . Alternatively, *structural* methods propose an indirect model-based approach, associating a latent ranking variable F_i with individual i . If $F_i > F_j$ then these *structural* methods infer that i dominates j . These latent variables are constructed to satisfy a set of a priori assumptions, and structural models attempt to estimate these latent ranks to best align with the behavior captured in W .

One clear advantage of model-based approaches is that W is a noisy realisation of the true underlying dominance ranking among animals. Methods which attempt to directly infer the ranking from W can therefore be unstable and unable to account for even small deviations from expected behavior. Model-based approaches, relying on *structural* methods, hold the potential to explore more complex behavioral patterns in such animal data and can also help generate hypotheses about this data which can be

further explored.

An important concept in dominance ranking is *linearity*. Under a strict linearity assumption, for any three individuals, i, j , and k , if i dominates j and j dominates k , then i is assumed to dominate k . In social network research, this closed triad relationship is also called *transitivity*. For *functional* methods, the linearity assumption intuitively follows from observational studies of group-living animals. However, phenomena that violate a strict linearity assumption are often observed. In these cases, *functional* methods aim to find a nearly linear ranking that is most consistent with the observed wins and losses. Meanwhile, in *structural* methods, the linearity assumption is not directly observable but is incorporated as a property of the latent parameter F . The goal for *structural* methods is to study the model that can mostly reflect the formation mechanisms of dominance hierarchy.

One popular functional model is the I&SI method of de Vries (1998). The I&SI method is a matrix-reordering method that identifies ordinal rankings of individuals that are most consistent with a linear hierarchy, by iteratively minimizing two criteria: the number of inconsistencies (I) and then, conditionally, the total strength of the inconsistencies (SI) without increasing I . The number of inconsistencies (I) is the number of pairs in which the lower-ranked individual wins more frequently than the higher-ranked individual in a given *win/loss* matrix, \tilde{W} ,

$$I = \sum_{i>j} \mathbb{1}_{\{\tilde{W}_{ij}>\tilde{W}_{ji}\}},$$

where $\mathbb{1}_{\{\cdot\}}$ is an indicator function. The matrix \tilde{W} is generated by reordering the original win/loss matrix W according to a ranking of the individuals. The *strength* of a single inconsistency is the absolute rank difference of the inconsistent pair. Then, the total strength of the inconsistencies (SI) is the sum of strengths of all inconsistencies in \tilde{W} ,

$$SI = \sum_{i>j} |i - j| \mathbb{1}_{\{\tilde{W}_{ij}>\tilde{W}_{ji}\}}.$$

An example is shown in Figure 1. The original *win/loss* matrix in the example is W , which corresponds to $I = 3$ and $SI = 7$. According to the I&SI ranking method, the matrix is reordered to yield \tilde{W} , the rightmost matrix in Figure 1, in which $I = 1$ and $SI = 3$. Intuitively, the I&SI method finds the order of the rankings that is most consistent with a linear hierarchy. Although such a perfect linear hierarchy usually does not exist, I&SI aims to find a ranking where any inconsistencies take place between individuals that are close in rank. In other words, the I&SI method is most likely to allow for inconsistent dyads near the diagonal.

This method suffers from the problem that the algorithm is not guaranteed to converge to a unique optimal solution (de Vries and Appleby, 2000). In particular, when there is a tie in the number of wins/losses ($W_{ij} = W_{ji} > 0$) or an unknown relationship (i.e., where there is little information, $W_{ij} = W_{ji} = 0$), the result highly depends on the choice of rules for assigning rankings. Another reason for the divergence is the method's reliance on only an asymmetric relationship between the number of wins and losses, instead of the absolute difference. Such a simplified binary dominance measure ignores important information in the data – the total number of fights. It is often observed that

$$\begin{array}{c}
\text{Recipient} \\
\begin{array}{ccccc}
1 & 2 & 3 & 4 & 5
\end{array} \\
\begin{array}{c}
\text{Actor} \\
\begin{array}{c}
1 \\ 2 \\ 3 \\ 4 \\ 5
\end{array}
\end{array}
\begin{pmatrix}
0 & 5 & 4 & 6 & 0 \\
0 & 0 & 0 & 0 & 1 \\
0 & 0 & 0 & 0 & 0 \\
0 & 3 & 0 & 0 & 0 \\
2 & 0 & 0 & 3 & 0
\end{pmatrix}
\end{array}
\longrightarrow
\begin{array}{c}
\text{Recipient} \\
\begin{array}{ccccc}
5 & 1 & 4 & 2 & 3
\end{array} \\
\begin{array}{c}
\text{Actor} \\
\begin{array}{c}
5 \\ 1 \\ 4 \\ 2 \\ 3
\end{array}
\end{array}
\begin{pmatrix}
0 & 2 & 3 & 0 & 0 \\
0 & 0 & 6 & 5 & 4 \\
0 & 0 & 0 & 3 & 0 \\
1 & 0 & 0 & 0 & 0 \\
0 & 0 & 0 & 0 & 0
\end{pmatrix}
\end{array}$$

Fig. 1. An example of a *win/loss* matrix and the corresponding reordered matrix according to the I&SI method. The entries shaded in red in the matrix are the *inconsistencies*, where the lower-ranked individual wins more frequently than the higher-ranked individual.

the distribution of dominance power exhibits a high discrepancy (Chase et al., 2002), such as when highly ranked animals win a larger number of fights against intermediately ranked animals than these intermediate animals win against lowly ranked animals. This is seen in a *win/loss* matrix with large variation in the values of W_{ij} , but an ordinal ranking from a binary dominance measure is not discriminative enough to demonstrate that. Williamson et al. (2016) provide an analysis of monopolization of the most dominant mouse in each cohort, which suggests the necessity for considering a real-valued score instead of the ordinal rank.

Winner-loser models are an important family of structural methods that explain the formation of linear dominance hierarchy (Lindquist and Chase, 2009). Commonly, the models assume an innate power parameter for each individual i , denoted as F_i (some models may assume a time-variant version, i.e. $F_i(t)$) (Bonabeau et al., 1999; Dugatkin, 1997; Hemelrijk, 2000). Although different models have their own specific formulations, common components they share are: an interaction probability and a dominance probability. Both are functions of innate power. The mathematical formulation of the models will not be discussed here, but some assumptions used in these model are of interest. One essential idea is the *winner effect*, the phenomenon in which an animal that has experienced previous wins will continue to win future aggressive interactions with increased probability. Although the extent and effectiveness of these winner effects remains unclear, evidence from experiments show that they exist and vary in different groups and species (Dugatkin, 1997; Dugatkin and Earley, 2003; Hsu and Wolf, 1999). Experimental evidence also shows patterns that are challenging to capture through winner-loser models, such as *bursting* and *pair-flips*. Bursting means that higher-rank animals often exhibit successive fighting of lower-rank ones in an extended period of time. Pair-flips describe the situation when a pair of animals exchange the direction of their aggressive acts before a stable dominance relationship is established. A potential model for learning a latent hierarchy should therefore be able to incorporate these characteristics. In Section 4 we describe several existing structural and functional models in detail, which we use for comparison with our proposed methods.

2.1. *Issues with conventional approaches*

In summary, although the current methods have certain advantages, they suffer from several issues. The use of an ordinal ranking alone may not be informative enough to describe the unequal distribution of dominance power which is commonly observed. Similarly, a more systematic solution is needed for modeling the temporal dynamics of the dominance hierarchy, instead of relying on empirical scores. The timestamps of these interactions are also likely to contain information about the particular hierarchy formation, and this time information should not be discarded. While existing structural models for this data provide much potential to understand the underlying drivers of animal behavior, methods to evaluate these models have been limited, as seen in Lindquist and Chase (2009). These models are generally not built under the statistical framework of a generative model and so it is hard to assess the goodness of fit of these models. The utilisation of a probabilistic generative model for latent ranking therefore provides the potential to rigorously assess model fit and help formalise scientific hypotheses. In the next section we will develop generative point process network models for this data, which we then compare with these existing methods in Section 4.

3. Latent ranking structured network point process models

In this section, we propose a hierarchy of probabilistic generative models to address common issues with conventional approaches, as discussed in the previous section. Inspired by theories on social hierarchy among group-living animals, there are various properties that we want to take into account when constructing the model: inconsistencies lying between the interactions and rankings, the time-evolving nature of the hierarchy dynamic, the winner effect, bursting and pair-flips phenomena, etc. Our model is designed to be interpretable and flexible enough to capture these key features of group-living animal behavior.

We first introduce the required notations on point process models and network data, leading to a model for network point processes (Section 3.1). We then propose three such network point process models based on latent (structural) rankings (Section 3.2). We motivate the development of each of these models in turn by examining the properties each model fails to capture in one cohort of mice interaction data (described in Section 4.4), using the inference procedure described in Section 4.2.

3.1. *Network point process models for animal interactions*

Animal aggressive interaction data is essentially network data, where the senders are the winners of the fights and the receivers are the losers. To consider the necessary information lying in the timestamps of interactions, we introduce point process models on networks. In this section, we start with notation and a discussion on point processes in general (i.e., for non-network data), with a focus on the Hawkes process. We then introduce the notation for network event arrival data and network point process models.

Point process models. Consider event arrival time data that consists of all event history up to a *final-observation* time T : $\mathcal{H}(T) = \{t_m\}_{m=0}^M$, where $t_0 = 0$, $t_M = T$, and M is the total number of events. An equivalent representation of this event history $\mathcal{H}(T)$ is

via a *counting process*, $N(t)$, where $N(t)$ is a right-continuous function that records the number of events observed during the interval $(0, t]$. The associated stochastic property is usually specified by its conditional intensity function $\lambda(t|\mathcal{H}(t))$ at any time $t \in (0, T]$, conditioning on current history $\mathcal{H}(t)$,

$$\lambda(t|\mathcal{H}(t)) = \lim_{\Delta t \rightarrow 0} \frac{\Pr(N(t + \Delta t) - N(t) = 1 | \mathcal{H}(t))}{\Delta t}.$$

This is the instantaneous expected rate of events occurring around a time t given the history. Inference on the intensity function is conducted by evaluating the likelihood function for a sequence of events up to time T , $\mathcal{H}(T)$, which can be expressed as (Daley and Jones, 2003)

$$\prod_{m=1}^M \lambda(t_m | \mathcal{H}(t_m)) \exp \left\{ - \int_0^T \lambda(s | \mathcal{H}(s)) ds \right\}. \quad (1)$$

A *Hawkes process* (Hawkes, 1971) is a linear self-exciting process that can explain bursty patterns in event dynamics. For a univariate model, the intensity function with exponential triggering function is defined as

$$\lambda(t) = \lambda_1 + \sum_{t_m < t} \alpha e^{-\beta(t-t_m)}, \quad (2)$$

where $\lambda_1 > 0$ specifies the baseline intensity, $\alpha > 0$ calibrates the instantaneous boost to the event intensity at each arrival of an event, and $\beta > 0$ controls the decay of past events' influence over time.

Network point process models. Consider a network consisting of a fixed set of N nodes, $V = \{1, 2, \dots, N\}$. For each directed pair of nodes (i, j) , the observations of interactions (fights) between them up to terminal time T includes the sender (winner) i , the receiver (loser) j and a sequence of event times $\mathcal{H}^{i,j}(T) := \{t_m^{i,j}\}_{m=0}^{M^{i,j}}$. Hence, a network Hawkes process model has a conditional intensity function for each pair (i, j) at time t given by $\lambda^{i,j}(t | \mathcal{H}^{i,j}(t))$. The likelihood of the interactions on the whole network is then

$$\prod_{i=1}^N \prod_{j \neq i}^N \prod_{m=1}^{M^{i,j}} \lambda^{i,j}(t_m^{i,j} | \mathcal{H}^{i,j}(t_m^{i,j})) \exp \left\{ - \int_0^T \lambda^{i,j}(s | \mathcal{H}^{i,j}(s)) ds \right\}.$$

3.2. Latent ranking structured models for network point processes

Motivated first by the *winner effect* reviewed in Section 2, we model the conditional intensity of interactions between a given sender receiver pair as a function of their event (winning) history. Although experimental observations cannot explicitly verify the extent or persistence of influence of historical events, the intensity formulation in the Hawkes process can help us model this *winner effect* flexibly. In a Hawkes process, α describes the extent to which previous wins influence the tendency to engage in a new fight. β represents the persistence – how fast this effect decays over time. A large β means that the winner effect decays quickly and only the most recent wins influence the tendency to engage in aggressive interactions at the present time.

For a directed pair (i, j) , the Hawkes process intensity is

$$\lambda^{i,j}(t) = \lambda_1^{i,j} + \alpha^{i,j} \sum_k \exp(-\beta^{i,j}(t - t_k^{i,j})),$$

where $\lambda_1^{i,j}$, $\alpha^{i,j}$ and $\beta^{i,j}$ are pair-wise parameters in Hawkes process. For all pairs, we introduce structure in the pair-wise parameters by assuming a latent rank variable, $f_i \in [0, 1]$, $i = 1, 2, \dots, N$. This is similar to the latent characteristic concept used in the winner-loser models (Lindquist and Chase, 2009) and the latent rank in the aggregate-ranking model (De Bacco et al., 2018) reviewed in Section 4.1.2. The latent rank variable essentially embeds each individual in a one-dimensional unobserved ranking space. We constrain the pair-wise intensity function by bounding the latent rank in order to avoid issues with model identifiability. This latent rank variable is a powerful feature of our model as it allows us to incorporate various model assumptions by specifying particular forms of the parameters $\lambda_1^{i,j}$, $\alpha^{i,j}$ and $\beta^{i,j}$ in the intensity function, as we will discuss in Section 3.2.1, 3.2.2 and 3.2.3.

3.2.1. Cohort Hawkes Process (C-HP) Model

In the first model, we assume a baseline intensity, λ_1 , and that the rate of decay for historical events, β , is constant across pairs. We structure the impact of historical events on each pair as a function of the pair's latent ranks f_i, f_j and parameters η , i.e. $\alpha^{i,j} := g_\eta(f_i, f_j)$. Inspired by the inconsistency and strength of inconsistency concepts in the I&SI method, we expect that the function $g_\eta(f_i, f_j)$ satisfies the following: (1) $g_\eta(f_i, f_j) > g_\eta(f_j, f_i)$ when $f_i > f_j$; (2) $g_\eta(f_i, f_j)$ is a decreasing function of $|f_i - f_j|$ when $f_i - f_j < 0$. Hence, we consider,

$$g_\eta(f_i, f_j) := \eta_1 f_i f_j \exp(-\eta_2 |f_i - f_j|) \text{logistic}(\eta_3 (f_i - f_j)),$$

where $\eta := (\eta_1, \eta_2, \eta_3)$. Figure 2-(a) shows the contour plot of $g_\eta(f_i, f_j)$, with $\eta_1 = 7.02$, $\eta_2 = 0.39$, and $\eta_3 = 1.66$, which are estimated values from real data analyzed in Section 4.4. Note that the x -axis in Figure 2-(a) is decreasing from left to right, in order to be consistent with the arrangement of a win/loss matrix, where the interactions between the most dominant pairs are displayed in the top left. We notice that the function takes higher values when $f_i > f_j$ (upper right triangle of Figure 2-(a)), compared to values when $f_i < f_j$ (lower left triangle of Figure 2-(a)). This ensures that aggressive behaviors are directed more frequently from a dominant individual towards a submissive individual, mirroring the *inconsistency* concept in I&SI method. The contour plot also shows that the form of this function agrees with the idea of minimizing the total strength of the inconsistencies in the I&SI method: it has a smaller value when $f_i < f_j$ and $|f_i - f_j|$ is larger (moving from the diagonal to lower left triangle of Figure 2-(a)).

Now, the intensity in the C-HP model is

$$\lambda^{i,j}(t) = \lambda_1 + g_\eta(f_i, f_j) \sum_k \exp(-\beta(t - t_k^{i,j})).$$

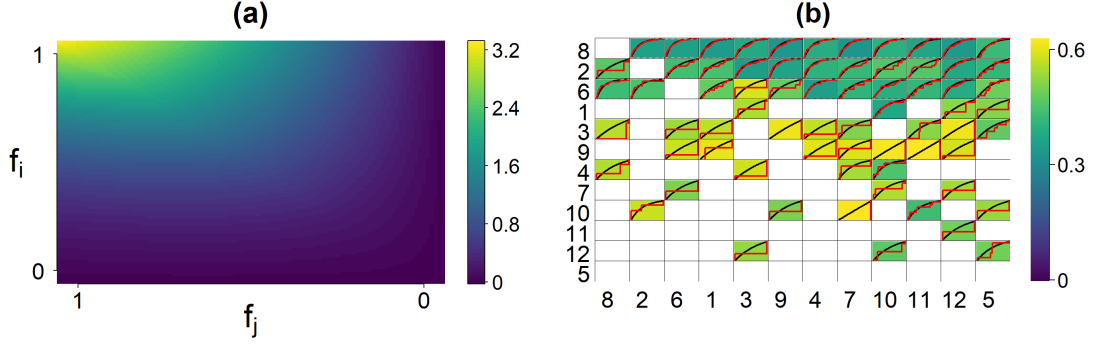


Fig. 2. (a) Contour plot for $\alpha^{i,j} := g_\eta(f_i, f_j)$ where $f_i, f_j \in [0, 1]$. (b) Matrix of K-S statistics after fitting the C-HP model to the real data (reordered by l&SI ranking). The rows and columns of this matrix correspond to senders and receivers of an agonistic behavior, respectively. Color shading reflects the values of the K-S test statistics. Red lines are empirical cumulative distribution functions of *rescaled-inter-event* times and black lines are cumulative distribution functions of exponential random variable with rate 1.

To assess the goodness-of-fit of point process models, according to the time rescaling theorem (Brown et al., 2002), we can test whether the *rescaled-inter-event* times $\{\Lambda_m := \int_{t_{m-1}}^{t_m} \lambda(s) ds\}_{m=1}^M$, are independently distributed following an exponential distribution with rate 1. We fit this model to data corresponding to interactions between a group of 12 mice, using the inference procedure of Section 4.2. We describe this data in more detail in Section 4.4. For each pair (i, j) , we conduct a Kolmogorov-Smirnov test on the *rescaled-inter-event* times $\{\Lambda_m^{i,j} := \int_{t_{m-1}^{i,j}}^{t_m^{i,j}} \lambda^{i,j}(s) ds\}_{m=1}^{M^{i,j}}$ and show the test statistics result in Figure 2-(b). The background color indicates the value of the K-S statistics. The values of these K-S statistics and the empirical cumulative distributions, such as on the sixth row and penultimate column, indicate a systematic lack of fit with this model. This suggests that this model does not adequately address individual baseline event intensities.

3.2.2. Cohort Degree Corrected Hawkes process (C-DCHP)

The cohort Hawkes process model (C-HP) model assumes a constant baseline rate λ_1 and is incapable of modeling the degree heterogeneity of the observed nodes. However, it can be observed from Figure 2-(b) that this model tends to consistently fit poorly for pairs which include certain individuals, for example those pairs in which the sender is individual 3 or the receiver is individual 7. To address this issue, we extend the C-HP model, allowing varying baseline intensity rates across pairs. We accommodate degree heterogeneity in the pairwise baseline rate $\lambda_1^{i,j}$ by introducing a set of non-negative out-degree-correction parameters γ_i and in-degree-correction parameters ζ_j , $i, j = 1, 2, \dots, N$. With the baseline rate defined as $\lambda_1^{i,j} = \gamma_i + \zeta_j$, we have the intensity function as

$$\lambda^{i,j}(t) = \gamma_i + \zeta_j + g_\eta(f_i, f_j) \sum_k \exp(-\beta(t - t_k^{i,j})).$$

This model introduces degree-correction parameters in the baseline rate of the C-HP model, hence, we refer to it as the cohort degree corrected Hawkes process model (C-DCHP). Figure 3 shows the baseline intensity matrix after fitting this model to the same cohort in Figure 2-(b). These estimates suggest that a model which allows more flexible intensities may indeed be needed to capture the heterogeneity in behavior across individuals. We can see that this degree correction successfully adjusts for less active actors or recipients. For example, consider individuals 8 and 9; as shown in Figure 3, their estimated λ_1^{ij} s are relatively large indicating that both individuals are more active in terms of interaction frequency; individual 9 tends not to initiate many fights and individual 8 tends not to be the recipient of many fights. Importantly, these differences in activity level are individual-level attributes and require separate consideration when we are interested in learning about dominance hierarchy from dyad-level agonistic interaction data. The resulting inferred ranks from the C-DCHP model for such individuals are more consistent with the ranking obtained from existing methods, compared to the inferred ranks from the C-HP model. Similarly, the resulting Kolmogorov-Smirnov statistics from estimating the goodness of fit of the C-DCHP model are on average smaller than those obtained for the original C-HP model, indicating improved performance in modeling the true underlying data generating process. However, the C-DCHP model consistently assigns a very large out-degree parameter value to the most dominant individual, as shown in Figure 3 and seen for all real data examples we consider. This complicates inference for the latent ranks of high-ranked individuals and leads to poor model performance for any interactions not involving this individual. In observed data, these interactions excluding this dominant individual more often exhibit more sporadic behaviour, with long periods where no events are observed, a feature we consider in the following model.

3.2.3. Cohort Markov-modulated Hawkes Process (C-MMHP)

In Wu et al. (2019), the Markov-modulated Hawkes Process (MMHP) is proposed to model sporadic and bursty event occurrences. The model utilises a latent two-state continuous-time Markov chain (CTMC) $Z(t)$ to better describe event dynamics. In state 1 (the *active* state), events occur according to a Hawkes process, while in state 0 (the *inactive* state), according to a homogeneous Poisson process. The transition of $Z(t)$ is modeled through an infinitesimal generator matrix with parameters $\{q_1, q_0\}$, such that,

$$Q = \begin{bmatrix} -q_1 & q_1 \\ q_0 & -q_0 \end{bmatrix}. \quad (3)$$

Hence, for one MMHP, the conditional intensity function given the latent Markov process $Z(t)$, history events $\mathcal{H}(t)$ and parameter set $\Theta = \{\lambda_0, \lambda_1, \alpha, \beta, q_1, q_0\}$ is

$$\lambda(t|Z(t), \mathcal{H}(t), \Theta) = \begin{cases} \lambda_0, & \text{when } Z(t) = 0, \\ \lambda_1 + \alpha \sum_k \exp(-\beta(t - t_k)), & \text{when } Z(t) = 1. \end{cases}$$

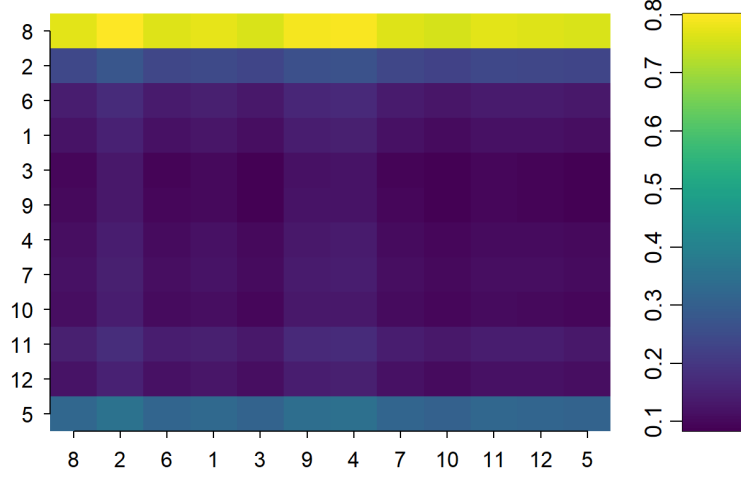


Fig. 3. Matrix of baseline rates $\lambda_1^{i,j}$ (reordered by I&S rankings). These degree corrected baseline rates allow for a more flexible node level model, clearly seen in the top row (a mouse which is involved in starting a large number of fights) and the bottom row (a mouse which does not start any fights but is often fought).

Implicitly, the intensity function has the form

$$\lambda_0 + (\lambda_1 - \lambda_0)Z(t) + \alpha Z(t) \sum_k \exp(-\beta(t - t_k)).$$

Thus, the latent process provides substantial flexibility in modeling the baseline rate as well as the extent of historical event influence.

We can readily extend this model to the network setting, where for each pair (i, j) , the intensity follows,

$$\lambda(t|Z^{i,j}(t), \mathcal{H}^{i,j}(t), \Theta^{i,j}) = \begin{cases} \lambda_0^{i,j}, & \text{when } Z^{i,j}(t) = 0, \\ \lambda_1^{i,j} + \alpha^{i,j} \sum_k \exp(-\beta^{i,j}(t - t_k^{i,j})), & \text{when } Z^{i,j}(t) = 1. \end{cases} \quad (4)$$

Here $\Theta^{i,j} := \{\lambda_0^{i,j}, \lambda_1^{i,j}, \alpha^{i,j}, \beta^{i,j}, q_1^{i,j}, q_0^{i,j}\}$ is the parameter set for pair (i, j) . $q_1^{i,j}$ and $q_0^{i,j}$ are the instantaneous transition probabilities for the latent CTMC $Z^{i,j}(t)$ of a pair (i, j) . $Z^{i,j}(t)$ are independent across pairs. The transition probability $q_1^{i,j}$ ($q_0^{i,j}$) represents the probability that pair (i, j) transitions out of the active (inactive) state and is modelled as a function of the latent ranks, f_i, f_j . To understand the behavior of these latent state transition parameters for each pair (i, j) , consider the stationary distribution of the latent CTMC, $Z^{(i,j)}(t)$. For an irreducible and recurrent CTMC $Z(t)$ with infinitesimal generator as shown in (3), a stationary distribution π satisfies $\pi^T Q = 0$ (Yin and Zhang, 2012). Hence for a pair (i, j) , the limiting behavior of their latent state transitions dictates that they spend $\frac{q_0^{i,j}}{q_0^{i,j} + q_1^{i,j}}$ of their time in the active state, and all remaining time in the inactive state. With the hope that if i dominates j , i.e. $f_i > f_j$, the pair (i, j)

will spend lots of time in the active state, we form the transition probabilities as,

$$q_1^{i,j} = \exp(-\eta_3 f_i)$$

$$q_0^{i,j} = \exp(-\eta_3 f_j).$$

Hence, when individual i is stronger than individual j , the directed pair (i, j) should be more likely to start and stay fighting (i.e. large $q_0^{i,j}$ and small $q_1^{i,j}$) than the pair (j, i) . This follows the *asymmetry* property of aggressive behavior in group animals. The limiting distribution of time spent in state 1 is $\text{Logistic}(\eta_3(f_i - f_j))$.

Given the latent process between pair (i, j) , $Z^{i,j}(t)$, we assume that $\beta^{i,j}$ is a constant β across pairs. As in the C-HP and C-DCHP models, we model the winner effect $\alpha^{i,j}$ as taking the form $\eta_1 f_i f_j \exp(-\eta_2 |f_i - f_j|)$. Like the C-DCHP, we again consider the degree correction described in the previous model here, giving $\lambda_0^{i,j} = \gamma_i + \zeta_j$. $\lambda_1^{i,j}$ is defined by

$$\lambda_1^{i,j} = \lambda_0^{i,j}(1 + w_\lambda),$$

for a common w_λ , to ensure that the base rate of the point process in the active state is greater than the inactive state. Hence we have the intensity from i to j given by

$$\lambda^{i,j}(t) = \lambda_0^{i,j} + (\lambda_1^{i,j} - \lambda_0^{i,j})Z^{i,j}(t) + \eta_1 f_i f_j \exp(-\eta_2 |f_i - f_j|)Z^{i,j}(t) \sum_k \exp(-\beta(t - t_k^{i,j})).$$

3.3. Model inference

Bayesian modeling. Throughout this paper, we adopt a Bayesian framework for our model inference. Assuming a prior distribution for the model parameters and given a model likelihood, the posterior distribution for quantities of interest can help us calibrate the uncertainty in the model. This is an important aspect of our current research strategy. First, we need tools that can quantify uncertainty in rank inference. For example, in Williamson et al. (2016), the analysis shows that the *pair-flips* phenomenon exists in some cohorts, which means that the direction of aggressive interaction changed over time. In a Bayesian modeling framework, we can naturally capture this effect through uncertainty in the model parameters: we suspect that individuals that are involved in pair-flip phenomena should have larger posterior variances for their latent ranks. Second, in each cohort, there always exists some pairs that have few or no interactions across the observation time window. A Bayesian framework can achieve robust inference in such conditions, with the assistance of prior assumptions and by borrowing strength from the data of other pairs. In this paper, we will use the Stan modeling language (Carpenter et al., 2017) to fit all models and to obtain posteriors samples for model parameters. We describe further details of our inference procedure in Section 4.2.

4. Results

4.1. Comparison Models

Before analysing the performance of our models on both real and simulated data, we first describe in detail existing methods used to analyse dominance behavior in animals, which

we shall use for comparison of inferred rankings. As described above, these methods can be broadly classified as *functional* and *structural*.

4.1.1. *Functional methods*

Along with the I&SI method, So et al. (2015) and Williamson et al. (2016) use the Glicko rating system to calculate temporal changes in dominance scores of each animal in each cohort. This is a dynamic paired comparison system that calculates a temporal sequence of cardinal scores based on the history of dyadic wins and losses (Glickman, 1999). All individuals start with the same initial rating. After each observed fight between a pair, the winner (or the loser) gains (or loses) points according to a decreasing function of the difference between their previous scores. In this case, fighting between pairs whose scores differ a lot will not result in significant changes in the system. The calculation of the Glicko score depends on a predefined constant, which determines the volatility of the score changes. Since scores are computed after each fighting event, this method can capture the temporal dynamics of the dominance hierarchy, although it does not account for temporal components, such as the time between events. Williamson et al. (2016) also provides a clear visualization of the change in the dominance score based on this method, where the emergence and stabilization of the hierarchy can be easily deduced from the graph. However, this method is ad-hoc in the sense that there are no theoretical rules for researchers to choose important key aspects of this method, including the initial rating, the decreasing function for changing a pair’s scores after an observed fight, or the constant controlling the volatility of score changes. Since the method focuses on summarizing the observations without any formal modeling, it can be hard to provide formal insights regarding the evolution of hierarchy dynamics. It is also not always clear how to draw a conclusion about the hierarchy structure from the visualization of the rating system.

4.1.2. *Structural methods*

Lindquist and Chase (2009) apply winner-loser models to real experimental data of hens and show the lack of fit between these models and the data. However, this procedure is qualitative only, by comparing simulation results from the models with the real data. The probabilistic generative models we proposed in Section 3 are able to capture these important animal behavior phenomena, including the *winner effect*, *bursting* and *pair-flips*. We also develop a corresponding statistical inference procedure which means that model-fitting can be assessed by rigorous statistical model diagnostics, rather than relying on simulations as in Lindquist and Chase (2009). We analyse our models using these diagnostics in Section 4.3 and Section 4.4.

A more recent structural model is De Bacco et al. (2018), which introduced a physics-inspired model to infer cardinal hierarchical rankings of individuals in directed networks. By assuming that individuals are more likely to interact with others of similar rank, they propose an optimization solution and a generative model to find real-valued ranks of individuals. For a pair (i, j) , with latent rank variables f_i and f_j , the aggregate-ranking model uses Poisson regression to model the aggregate counts between the pair over the entire observation period, denoted as $N_{i,j}$, as a function of the difference in their ranks.

This is essentially the counting process evaluated at time T , $N^{i,j}(T)$, ignoring the exact event times. However, the only information used in the model is the existence and direction of the interactions in the network. We refer to this model as the *aggregate-ranking* model. Only using the aggregate counts of interactions makes it hard to address phenomena like the *winner effect*, *bursting* and *pair-flips* mentioned in Lindquist and Chase (2009). Event time data which records when the aggressive behaviors occur is highly detailed and contains information needed to describe the important phenomena mentioned earlier.

4.2. Model implementation

To perform inference for each of these models we perform Bayesian inference using the Stan programming language (Stan Development Team, 2020). We impose weakly informative priors for the model parameters where possible. In particular, for each model we use $\text{logN}(0, 1)$ priors on η_1, η_2, η_3 , $U[0, 1]$ priors for f and a $\text{logN}(0, 2)$ prior for w_λ in the C-MMHP model, to ensure that the rate in the active state is greater than in the inactive state. For the degree corrected models we place $\text{InvGamma}(3, 0.5)$ priors on γ and ζ . Full details of the inference procedure to infer the latent states of the C-MMHP model are given in Wu et al. (2019).

4.3. Synthetic results

We first wish to validate our proposed models using simulated data where we aim to recover the known latent ranking vector. To compare the three proposed models, we simulate 50 independent C-MMHPs with five nodes and parameters with values $\gamma = (0.01, .02, .03, .06, .07)$, $\zeta = (.075, .06, .05, .03, .02)$, $\eta_1 = 2.5, \eta_2 = 0.6, \eta_3 = 0.8, \beta = 1.5$, latent rank $f = (0.1, 0.2, 0.4, 0.7, 0.9)$, and common $\lambda_1 = 0.15$. By fitting the synthetic data with our previous three models, we can obtain the inferred latent ranks as shown in Figure 4 - (a). Inference using C-MMHP best recovers the true latent ranks, with the C-HP and C-DCHP showing considerably more uncertainty in their estimates. Figure 4 - (b) shows an example of estimated intensity for one pair of individuals in one simulated process, indicating that the C-HP and C-DCHP models cannot capture the true intensity as well as the C-MMHP model, showing substantial underestimation of the intensity during the active state.

To further explore this lack-of-fit in the C-HP and C-DCHP models, we again utilize the time rescaling theorem (Brown et al., 2002) to diagnose model misspecification. With the estimated intensity for each pair $\hat{\lambda}^{(i \rightarrow j)}$, we use a KS test to test whether the *rescaled-inter-event* times are distributed as exponential random variables with rate 1. The KS statistics of the process for each pair with respect to the three previous models and true intensity are plotted in Figure 5-(a). C-HP and C-DCHP both demonstrate a similar fit compared to C-MMHP, although there are several pairs where the C-HP and C-DCHP models demonstrate a slightly larger lack of fit. We can also compare the inferred ranking from each of these models and the comparison models discussed previously with the known true ranking. We summarize this using the Spearman rank correlation between the estimated ranking obtained from each method and the true ranking, as shown in Fig 5-(b). We note that the C-MMHP model recovers the exact

ranking in all but one simulation, with the C-HP and C-DCHP models also performing well but showing more variability. As a structural method, the I&SI model recovers the true ranking reasonably well.

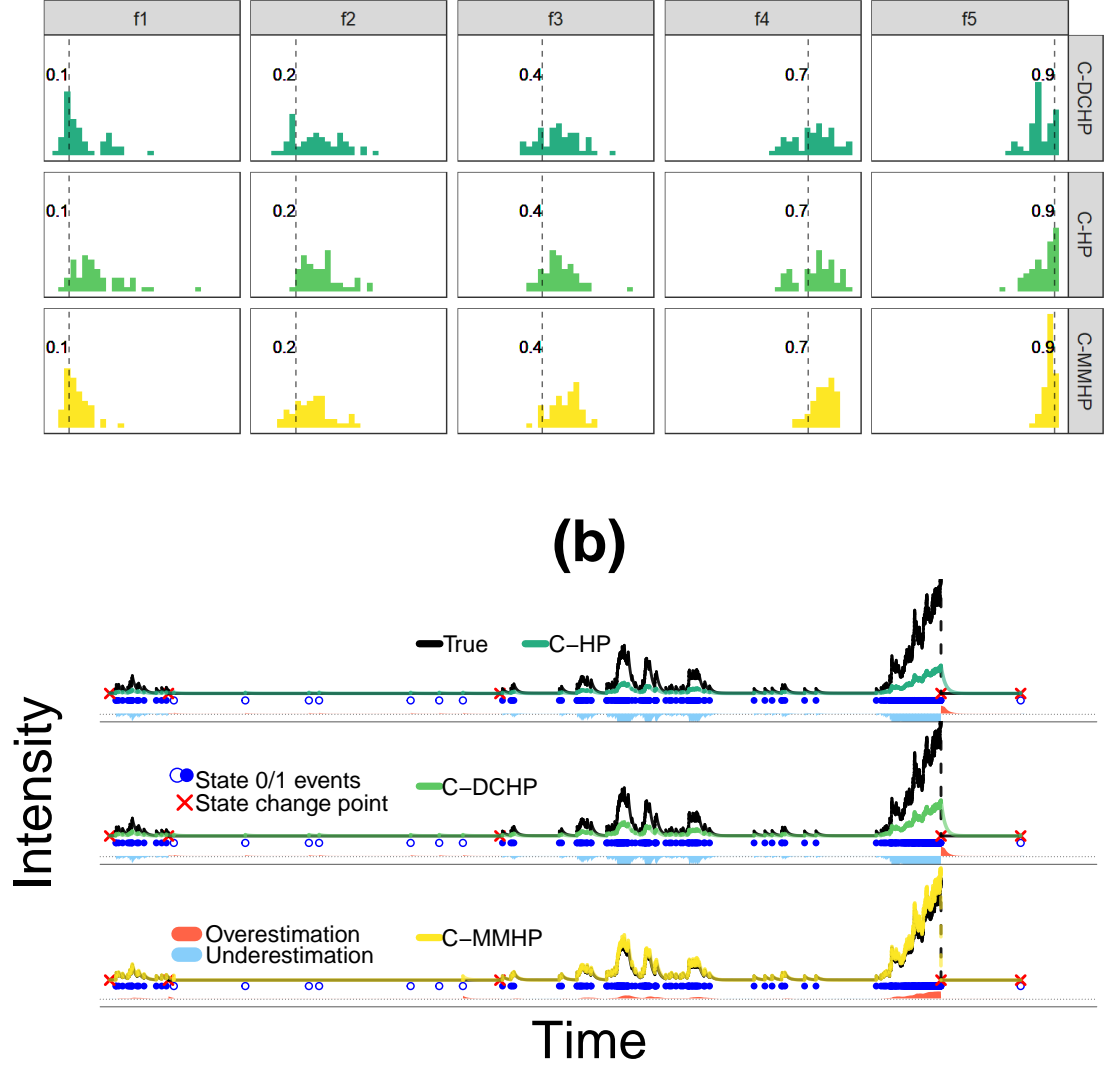


Fig. 4. Simulation results. (a) Posterior inference of latent rank variable $f_i, i = 1, \dots, 5$ by C-HP, C-DCHP and C-MMHP. Each value is the posterior mean for f_i inferred from 50 independent simulations from the same underlying C-MMHP model. The black vertical line is the true value. (b) Inferred intensity for one pair of individuals in one simulation using three models. Here the red/blue shaded area underneath shows the magnitude of the error in the estimation of the intensity.

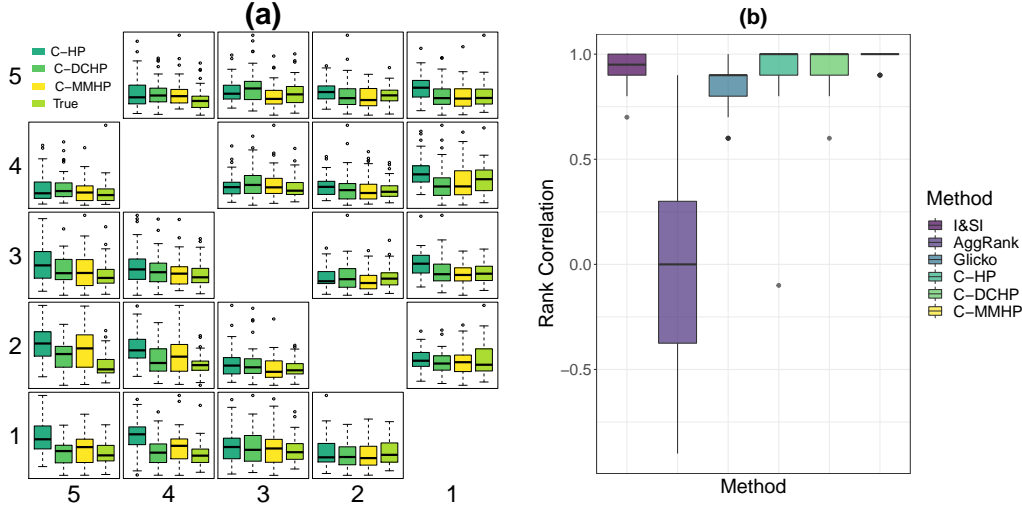


Fig. 5. (a) Shows K-S test statistics for point process model diagnosis with respect to three models and ground truth. (b) Shows the Spearman rank correlation between the inferred ranking from each of these models, along with existing methods, and the known true ranking.

4.4. Real data results

We next fit our models, C-HP, C-DCHP and C-MMHP to the ten mice cohorts studied by Williamson et al. (2016), which consisted of placing each cohort of twelve male mice in a large custom built vivarium. Intensive behavioral observations were conducted for one to three hours per day during the dark cycle over twenty-one consecutive days. Trained observers recorded all occurrences of the behaviors (including fighting, chasing, mounting, subordinate posture and induced-flee). The details of each behavioral event are also recorded, including the actor initializing the behavior, the recipient of the behavior, time stamp and location.

Using various measurements in social hierarchy analysis and social network analysis, Williamson et al. (2016) demonstrates that these mice cohorts form significantly linear social dominance hierarchies. The work also examines the temporal changes in the mice social hierarchy and shows that in most of the ten cohorts, the dominance hierarchies emerge rapidly and become stable by the end of the second week. Although results of the quantitative analysis are thoroughly discussed and the patterns in the temporal dynamics are summarized qualitatively, there are still observations in some cohorts that disagree with the authors' speculations. Additionally, there are questions that remain unanswered, e.g., what mechanism is behind the establishment of hierarchies, why sometimes agnostic interactions occurred between pairs in an uncommon direction, how inequitable the distribution of individuals' dominance power is, etc. We also compare the results from fitting the following models to this data: a dynamic social network in latent space model, and a Markov-modulated Hawkes process with independent network structure.

Dynamic social network in latent space model (DSNL) (Sarkar and Moore, 2006). This model is constructed for dynamic network data with binary links which is observed in discrete time steps. The model associates each node in the network with a latent space variable that can move in discrete time, and specifies that the move is Markovian. For node i at discrete time d , the latent variable is denoted as $f_i^{(d)}$. We tailor this model to our observed mice interaction data by changing the binary link assumption in the original model to allow for aggregate counts by using a Poisson link instead of a logistic link. We construct discrete time steps to be the ending time of each day in the observation time window, i.e. $t^{(d)}$. Hence, for each pair (i, j) , we have the count of their interactions during day d , $N_d^{i,j} := N^{i,j}(t^{(d)}) - N^{i,j}(t^{(d-1)})$, where $N^{i,j}(t)$ is the counting process for pair (i, j) evaluated at time t . The details of this model will be omitted here.

Markov-modulated Hawkes process with independent network structure (I-MMHP) (Wu et al., 2019). In this model, we assume that the intensity function as in (4) allows for different parameter values $\Theta^{i,j}$ across pairs. The independent structure of the parameters in this model is less constrained than our C-MMHP model, where we consider network structure between nodes to learn latent rankings.

Summary measures for evaluating model performance. Our real data analysis results will be summarized from four different perspectives: inference for the latent ranks, prediction performance, additional insights available through the C-MMHP model, and finally residual analysis of the point process models. We compare the results of the C-HP, C-DCHP and C-MMHP models under the first three of these perspectives. Because the nature of the three other comparison models - aggregate-ranking, DSNL and I-MMHP - differs, they are fitted and compared from different perspectives. The aggregate-ranking model (and also the I&SI method we discussed previously) estimates a static ranking and will be evaluated in terms of inference for the latent ranks only. The I-MMHP is a point process model and can be evaluated using the same point process methods as our latent ranking point process models. However, the I-MMHP cannot be used to infer a latent ranking. Finally, both the DSNL and I-MMHP models can perform prediction of events (or event counts) and can serve as comparison models in the prediction performance section.

4.4.1. Inference on latent rank

We fit the C-HP, C-DCHP, C-MMHP and aggregate-ranking models to our data of ten cohorts separately. Figure 6-(a) shows the relationship between I&SI rank and posterior draws of latent ranks using our three models and aggregate-ranking model in one such cohort - cohort 5. Here a boxplot which is more diagonal from top left to bottom right indicates that the ranking method is more consistent with the I&SI method. C-MMHP agrees with I&SI well, is better able to distinguish between lower ranked mice than the aggregate ranking method, and is better at identifying the top ranking mouse than C-DCHP. It also appears to include a reasonable amount of uncertainty. To summarize results across all of the 10 cohorts, we use the posterior mean to estimate the latent rank and compute the Spearman rank correlation between the inferred latent rank and the

I&SI rank. Figure 6-(b) shows the summary of the rank correlation for all ten cohorts, where C-MMHP outperforms the other point process models consistently and gives a similar result to the aggregate ranking method. It is not surprising that the aggregate-ranking model performs well here as it uses the same data (the win/loss matrix) as the I&SI method, ignoring the time component.

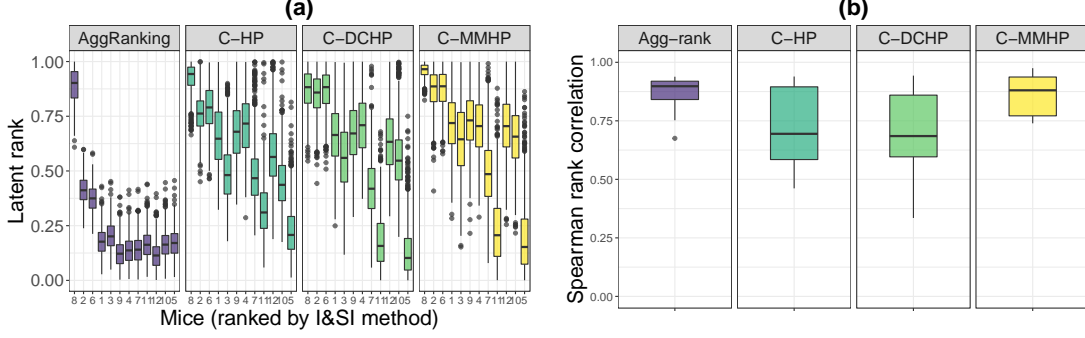


Fig. 6. Real data fitting results. (a) Comparison of rank inference using different model with I&SI rank for one cohort. (b) Summary of Spearman rank correlation between model inferred ranks and I&SI rank for all cohorts.

4.4.2. Prediction

We can also use posterior predictive distributions to validate the models considered. For each model, we split the data into two time periods: (1) the first 15 days of data, $\mathcal{H}^{i,j}(t^{(15)})$, where $t^{(d)}$ is the ending observation time for the d -th day, which is used to estimate the model and (2) a prediction window from day 15 to day $t^{(d)}$, for $d = 16, \dots, 21$, the remaining observation period, which allows us to compare models across different prediction horizons. For each prediction horizon $t^{(d)}$, we generate a predicted point process separately over the time period $t^{(15)}$ to $t^{(d)}$, given each posterior draw of parameters and the historical events in the first 15 days. Hence, the predicted counting process $\hat{N}^{i,j}(t)$ is constructed by generating processes in each prediction period and adding these to the true process in the model-fitting period. For each prediction horizon and model, we generate 1000 posterior processes, corresponding to 1000 posterior draws from the posterior distribution for the model parameters. Following Sarkar and Moore (2006), we can also make predictions over these same time windows using the DSNL model.

Two aspects of the predictions are evaluated, the accuracy of predictions for the interaction counts and the prediction of the rankings.

For each point process model and for each different prediction horizon $d = 16, \dots, 21$, the number of total interactions for pair (i, j) during the prediction period can be estimated by $\tilde{N}^{(i,j)}(t^{(d)}) - N^{(i,j)}(t^{(15)})$, where $\tilde{N}^{(i,j)}(t^{(d)})$ is the average count of interactions across 1000 posterior processes. We arrange the prediction counts in a matrix $\hat{A}^{(d)}$ such that each (i, j) entry is the predicted number of interactions for pair (i, j) from the end

of the 15th day until the d th day. To quantify the accuracy of these predicted counts, we calculate the Frobenius norm of the difference between the estimated and real interaction matrix $A^{(d)}$,

$$\|\hat{A}^{(d)} - A^{(d)}\|_F.$$

The smaller the Frobenius norm, the closer the model’s predictions of the interaction counts are to the observed data. Figure 7-(a) summarizes the result across all cohorts, by taking the median predicted counts for each pair across each of 1000 posterior draws. I-MMHP performs poorly since it does not take into account the dependence between nodes due to the underlying network structure and thus struggles to make accurate predictions across the whole network. The C-MMHP and C-HP models provide the best predictions of interaction counts, with the smallest Frobenius norms across all prediction horizons, with C-MMHP outperforming the C-HP model.

We also infer the predicted rank of individual i at prediction time $t^{(d)}$ by introducing the out-degree intensity

$$\hat{\lambda}_i(t^{(d)}) = \sum_j \hat{\lambda}^{i,j}(t^{(d)}).$$

The Glicko score ranking system serves as a bench mark for us to compare to, as it is a dynamic score. We compute the Spearman rank correlation of our inferred rank with the Glicko score at the end of the prediction day. Figure 7-(b) summarizes the result for all cohorts. The C-MMHP model predicts the ranks most accurately with rank correlation close to 1, with the unconstrained I-MMHP model also performing well in this scenario.

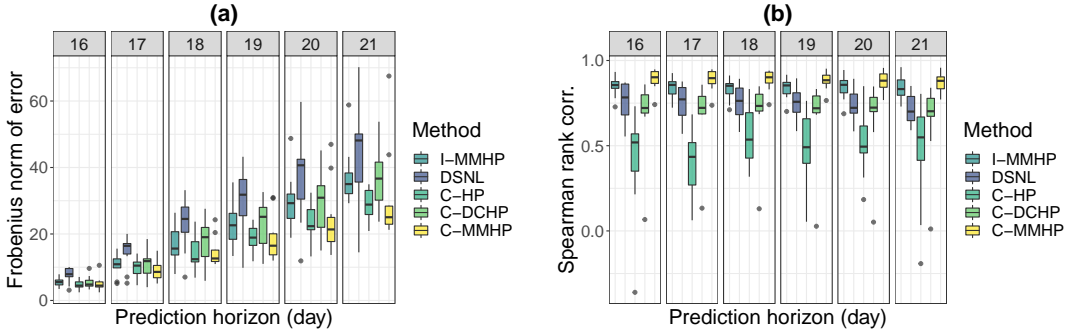


Fig. 7. Prediction of events and rank. (a) Frobenius norm of predicted error for all cohorts, using the median predicted count for each model for each cohort on each day. (b) Summarize the Spearman rank correlation of predicted rank for all cohorts, where each cohort is predicted by the posterior mean of $\hat{\lambda}_i(t^{(d)})$.

Our posterior predictive processes can even be used to forecast the Glicko scores over future prediction windows, since we obtain the full event history from the generated process. In contrast, the DSNL model can only provide day-level predictions, as we have evaluated in previous discussions. Figure 8-(a) shows the prediction of Glicko scores over days 19-21 when fitting the data in the first 18 days to the C-MMHP model. Our prediction bands can forecast temporal trends of Glicko ratings in the real data and provide an appropriate representation of the uncertainty in these predictions, which we

illustrate in Figure 8-(a). While these prediction bands show some mean reversion not seen in the true rankings, they correctly identify the highly ranked nodes and capture the groups of rankings that seem to have formed for this cohort. Being able to predict rank evolution over time is not possible using existing methods and this could be of use in the experimental design of these studies to guide data collection, such as the ability to isolate mice who would be expected to rank similarly in the original group.

4.4.3. State separation from the C-MMHP model

Additionally, since our C-MMHP model can separate interactions into active and inactive states, such separation can serve as a preprocessing step for the data. We first fit the C-MMHP model to the data for one cohort and classify the interactions into active and inactive states according to the estimated latent Markov process. The two types of interactions can then be fitted separately using other animal behavior models. Wu et al. (2019) shows that the interactions in the active state more closely follow a linear hierarchy, as compared to the set of all interactions or the set of inactive interactions; this provides an explanation for the *pair-flips* phenomenon. During the active state, pairs are engaging in aggressive interactions and actively trying to navigate the social hierarchy, while in the inactive state, the interactions are more or less random and lack specifically directed aggression as in the active state. As an example, we fit the DSNL model to the set of overall events, active events and inactive events separately, and calculate the Spearman rank correlation between the latent ranks for each day as estimated by the DSNL model and the Glicko ratings at the end of each day. Figure 8-(b) shows these rank correlations on each day for the three sets of interactions. This suggests that the set of active interactions provides a more informative and more concise perspective of how the linear hierarchy is established, and hence can improve the power of the DSNL model in terms of the inference for the underlying rankings.

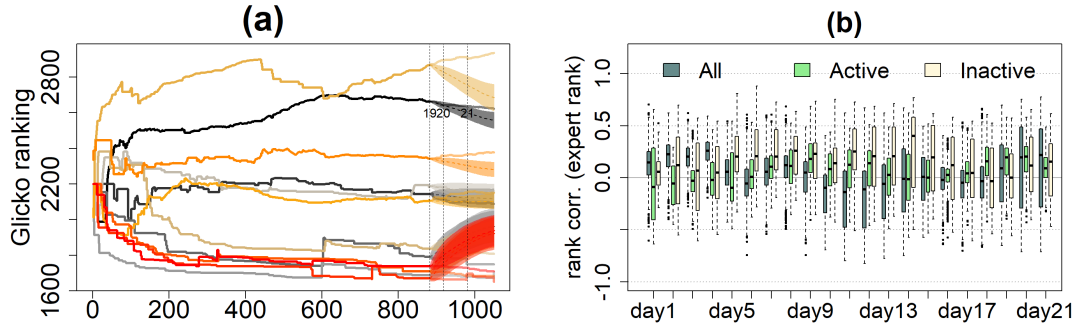


Fig. 8. Further results on C-MMHP. (a) Glicko score ranking prediction of last three days using posterior draws, after fitting the first 18 days data in C-MMHP. True Glicko score ranking of all the time period is shown with the solid colored line, while the posterior prediction mean is in dashed line and one standard deviation is plotted in shaded color. (b) Rank correlation between DSNL inferred latent rank and Glicko score ranking for each day in one cohort. Three colored bar indicated the performance of three inferred rankings conducted on the overall interactions, active and inactive respectively.

4.4.4. Residual analysis

For point process models on a social network, model checking via residual analysis is critical, aiding in identification of when and where the lack-of-fit in the model comes from. Given a network point process model with inferred intensity $\hat{\lambda}^{i,j}(t)$ for all directed pairs (i, j) , the Pearson residual can measure the fit of the estimated intensity to the data and is calculated as

$$\text{PR}_{i,j}(T) = \sum_{t_m^{i,j}} \frac{1}{\sqrt{\hat{\lambda}^{i,j}(t_m^{i,j})}} - \int_0^T \sqrt{\hat{\lambda}^{i,j}(s)} ds.$$

This is a rescaled residual with mean 0 and variance T . In the network setting, the Pearson residual is more informative compared to a raw residual, since different pairs may have various activity levels (Wu et al., 2020). Figure 9-(a) displays the Pearson residual for one cohort after fitting our three models and I-MMHP. The I-MMHP model yields small negative residuals for all observed pairs, with unsurprisingly smaller residual values than the more constrained comparison models. The C-HP model shows large positive residuals for interactions originating from the highest ranked mouse which the C-DCHP corrects for, although it results in almost all negative residuals, indicating systematic overfitting in this case. In contrast the C-MMHP model shows small positive and negative residuals, indicating little remaining structure. The C-MMHP model shows the closest performance to the unconstrained I-MMHP model.

5. Discussion

In this paper, we propose a statistical model that can uncover latent social dominance hierarchy among a group of animals from interaction event times. This model can serve as an important tool in animal aggressive behavior analysis. To accomplish this, we formalize a point process model for continuous-time directed social network data. Three such models are developed: the cohort Hawkes process model (C-HP), the cohort degree corrected Hawkes process model (C-DCHP) and the cohort Markov-modulated Hawkes process model (C-MMHP). The Hawkes process incorporates the winner effect and bursting patterns of aggressive behaviors, which are regularly observed in patterns of aggressive interaction across animal species. The degree correction allows the model to better capture individual level heterogeneity that is commonly observed in data of this form. Finally, Markov-modulation accounts for pair-flip situations and allows for asymmetry in interactions between pairs of animals, by separating these interactions into active and inactive states. Performing inference for these models in the Bayesian paradigm allows us to accurately quantify the uncertainty in the inferred rankings and to better infer the ranking of nodes involved in few interactions, components that have been lacking in existing models for animal ranking.

The simulation study demonstrates that inferences from these models are reasonable and that the true ranking of nodes can be recovered. The mice cohort study serves as a real data example and demonstrates that the C-MMHP model performs best overall, in terms of latent rank inference, prediction of both events and rank over time and residual diagnostics. This C-MMHP model can also be used to simulated future events, which could aid in designing studies of this form. Similarly, the state separation available in

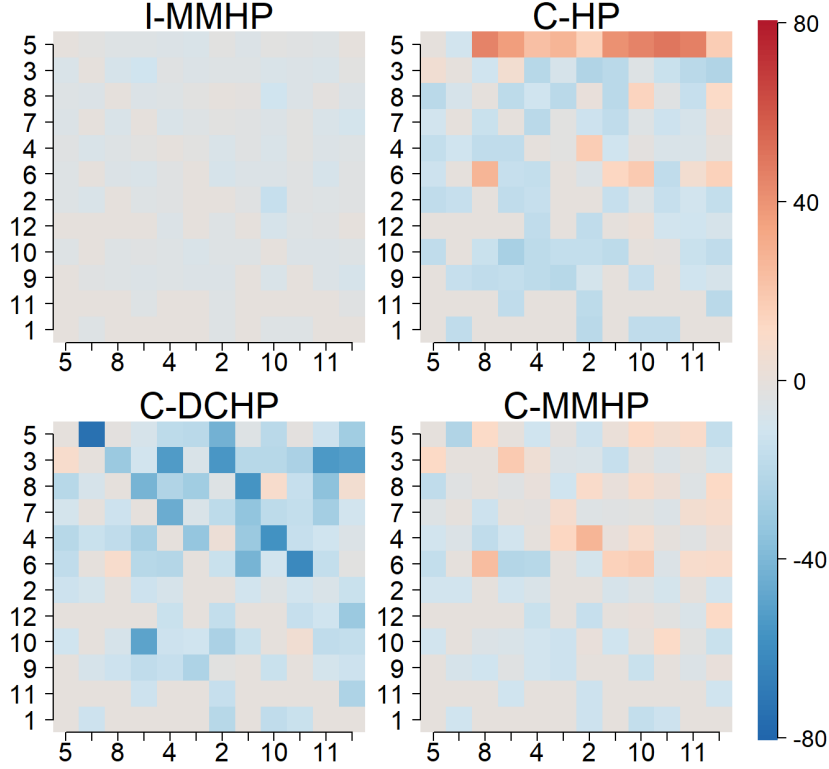


Fig. 9. Comparison of Pearson residual matrix using different models for one cohort (the matrix is reordered by I&SI rank). (b) Shows the corresponding matrix structure scores for both positive and negative residuals for each of the 10 mice cohorts.

the C-MMHP model could lead to additional insights in conjunction with other models for animal behavior.

In the future, our model can be extended to incorporate the loser effect and bystander effect (Chase and Seitz, 2011) within the Hawkes process intensity function. The loser effect means that an animal that has lost in earlier contests has an increased probability of losing subsequent contests with other individuals. The bystander effect describes the situation where an animal's behavior might be influenced by observing an interaction or contest between two other animals. The extent of each effect can be estimated through a multivariate Hawkes process. The existence of such effects could be tested through the limiting distribution in Chen et al. (2017). So et al. (2015) raises a question about the causal relationship between aggressive behavior and gene expression. It is feasible to integrate these elements in our model by modeling the baseline intensities as a function of covariates that correspond to gene expression. Similarly, the model we have proposed here is a special case of a latent space model. Latent space models are an important tool in social network analysis and have been widely used in modeling both static network (De Bacco et al., 2018; Hoff, 2005; McCormick and Zheng, 2015) and dynamic network

(Sarkar and Moore, 2006; Sewell and Chen, 2015) data. Although latent space models of discrete-time dynamic networks have been considered (Kim et al., 2018), there has been little work in the context of continuous time dynamic networks, and this remains an area for future research.

Acknowledgement

This material is based on research sponsored by DARPA agreement number D17AC00001. The content of the information does not necessarily reflect the position or the policy of the Government, and no official endorsement should be inferred.

Data and Code

All data and code used in this paper will be made available in a public repository.

References

- Bonabeau, E., Theraulaz, G., and Deneubourg, J.-L. (1999). Dominance orders in animal societies: the self-organization hypothesis revisited. *Bulletin of mathematical biology*, 61(4):727–757.
- Brown, E. N., Barbieri, R., Ventura, V., Kass, R. E., and Frank, L. M. (2002). The time-rescaling theorem and its application to neural spike train data analysis. *Neural computation*, 14(2):325–346.
- Carpenter, B., Gelman, A., Hoffman, M. D., Lee, D., Goodrich, B., Betancourt, M., Brubaker, M., Guo, J., Li, P., and Riddell, A. (2017). Stan: A probabilistic programming language. *Journal of statistical software*, 76(1).
- Chase, I. D. and Seitz, K. (2011). Self-structuring properties of dominance hierarchies: a new perspective. In *Advances in genetics*, volume 75, pages 51–81. Elsevier.
- Chase, I. D., Tovey, C., Spangler-Martin, D., and Manfredonia, M. (2002). Individual differences versus social dynamics in the formation of animal dominance hierarchies. *Proceedings of the National Academy of Sciences*, 99(8):5744–5749.
- Chen, S., Shojaie, A., Shea-Brown, E., and Witten, D. (2017). The multivariate hawkes process in high dimensions: beyond mutual excitation. *arXiv preprint arXiv:1707.04928*.
- Daley, D. J. and Jones, D. V. (2003). *An Introduction to the Theory of Point Processes: Elementary Theory of Point Processes*. Springer.
- De Bacco, C., Larremore, D. B., and Moore, C. (2018). A physical model for efficient ranking in networks. *Science advances*, 4(7):eaar8260.
- de Vries, H. (1998). Finding a dominance order most consistent with a linear hierarchy: a new procedure and review. *Animal Behaviour*, 55(4):827–843.

- de Vries, H. and Appleby, M. C. (2000). Finding an appropriate order for a hierarchy: a comparison of the i&si and the bbs methods. *Animal Behaviour*, 59(1):239–245.
- Drews, C. (1993). The concept and definition of dominance in animal behaviour. *Behaviour*, 125(3):283–313.
- Dugatkin, L. A. (1997). Winner and loser effects and the structure of dominance hierarchies. *Behavioral Ecology*, 8(6):583–587.
- Dugatkin, L. A. and Earley, R. L. (2003). Group fusion: the impact of winner, loser, and bystander effects on hierarchy formation in large groups. *Behavioral Ecology*, 14(3):367–373.
- Glickman, M. E. (1999). Parameter estimation in large dynamic paired comparison experiments. *Journal of the Royal Statistical Society: Series C (Applied Statistics)*, 48(3):377–394.
- Hawkes, A. G. (1971). Spectra of some self-exciting and mutually exciting point processes. *Biometrika*, pages 83–90.
- Hemelrijk, C. K. (2000). Towards the integration of social dominance and spatial structure. *Animal behaviour*, 59(5):1035–1048.
- Hoff, P. D. (2005). Bilinear mixed-effects models for dyadic data. *Journal of the american Statistical association*, 100(469):286–295.
- Hsu, Y. and Wolf, L. L. (1999). The winner and loser effect: integrating multiple experiences. *Animal Behaviour*, 57(4):903–910.
- Kim, B., Lee, K. H., Xue, L., Niu, X., et al. (2018). A review of dynamic network models with latent variables. *Statistics Surveys*, 12:105–135.
- Lindquist, W. B. and Chase, I. D. (2009). Data-based analysis of winner-loser models of hierarchy formation in animals. *Bulletin of mathematical biology*, 71(3):556–584.
- McCormick, T. H. and Zheng, T. (2015). Latent surface models for networks using aggregated relational data. *Journal of the American Statistical Association*, 110(512):1684–1695.
- Sarkar, P. and Moore, A. W. (2006). Dynamic social network analysis using latent space models. In *Advances in Neural Information Processing Systems*, pages 1145–1152.
- Sewell, D. K. and Chen, Y. (2015). Latent space models for dynamic networks. *Journal of the American Statistical Association*, 110(512):1646–1657.
- So, N., Franks, B., Lim, S., and Curley, J. P. (2015). A social network approach reveals associations between mouse social dominance and brain gene expression. *PloS one*, 10(7):e0134509.
- Stan Development Team (2020). RStan: the R interface to Stan. R package version 2.21.2.

- Williamson, C. M., Lee, W., and Curley, J. P. (2016). Temporal dynamics of social hierarchy formation and maintenance in male mice. *Animal Behaviour*, 115:259–272.
- Wu, J., Smith, A. L., and Zheng, T. (2020). Diagnostics and visualization of point process models for event times on a social network. *arXiv preprint arXiv:2001.09359*.
- Wu, J., Ward, O., Zheng, T., and Curley, J. (2019). Markov-modulated hawkes processes for sporadic and bursty event occurrences. *arXiv: 1903.03223*.
- Yin, G. G. and Zhang, Q. (2012). *Continuous-time Markov chains and applications: a singular perturbation approach*, volume 37. Springer.